

# CP Violation at ATLAS

Adam Barton  
Lancaster University  
For ATLAS collaboration  
**DISCRETE 2012**



# Introduction

- One of the main tasks in particle physics today is to test Standard Model predictions
- The observed baryon asymmetry in the universe suggests the SM underestimates CPV, giving a strong motivation for experimental investigation
- One of the promising decays where New physics is expected to alter a CP violation is the  $B_s \rightarrow J/\psi\phi$  channel. The SM predicts a small value of CPV phase  $\varphi_s \approx -2\beta = -0.0368 \pm 0.0018$  rad
- ATLAS has published the first of a series of measurements of CP violation in  $B_s \rightarrow J/\psi\phi$  (arXiv:1208.0572, accepted by J. High Energy Phys.)

## B Physics potential at ATLAS

- There is a large beauty production cross-section at the LHC when running at 7 TeV and a very high luminosity (currently at  $\sim 8 \times 10^{33} \text{cm}^{-2} \text{s}^{-1}$  in 2012)
- The ATLAS detector features:
  - High precision vertex resolution
  - Ability to reconstruct exclusive final states with good resolution
  - Flexible trigger scheme
  - Ability to reconstruct decays with high levels of pile-up (multiple pp interactions read out at once)

# The ATLAS detector



Muon Spectrometer (MS)  
0.5 - 2 T toroid magnet,  
Four detector technologies  
Dedicated tracking  
chambers

Three Level trigger System:  
L1(Hardware) + HLT (L2 + EF  
software)  
B physics mostly utilises the  
muon triggers

LHC p-p run for 2011 finished, after  
operating at 7 TeV  
8 TeV run for 2012 has also completed  
but data not analysed for CPV yet

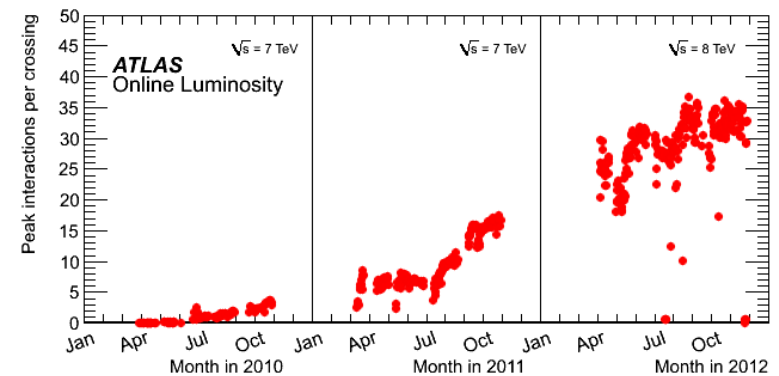
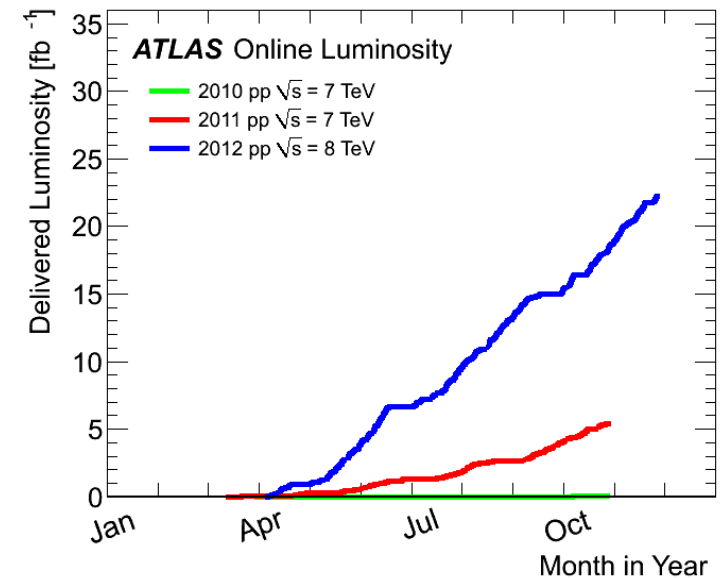
Acceptance in pseudo-rapidity  
up to 2.5 for Inner Detector, up  
to 2.7 for muon spectrometer

Good muon momentum resolution  
provided by Inner Detector combined with  
Muon Spectrometer measurement

Inner Detector(ID):  
Si Pixels + Si strips (SCT) +  
Transition Radiation  
Tracker(TRT)  
2T solenoid field

# ATLAS data collection

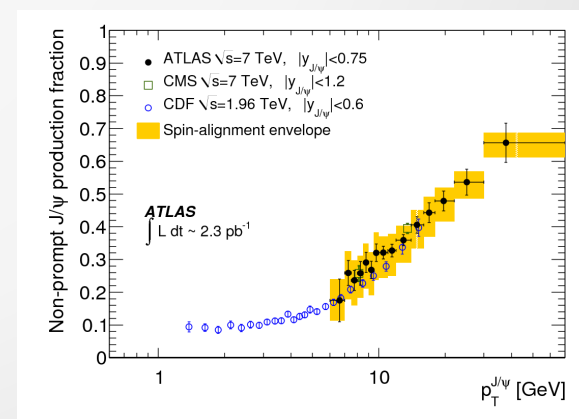
- In 2010 ATLAS and LHCb collected similar integrated luminosities
- Since 2011 ATLAS/CMS benefited from being able to record nearly the full luminosity delivered by LHC, ATLAS recorded luminosity  $\sim 5.2 \text{ fb}^{-1}$  in 2011
- To benefit from the high luminosity special consideration must be paid attention to B-physics triggers and vertexing performance with regard to increasing pileup in events.



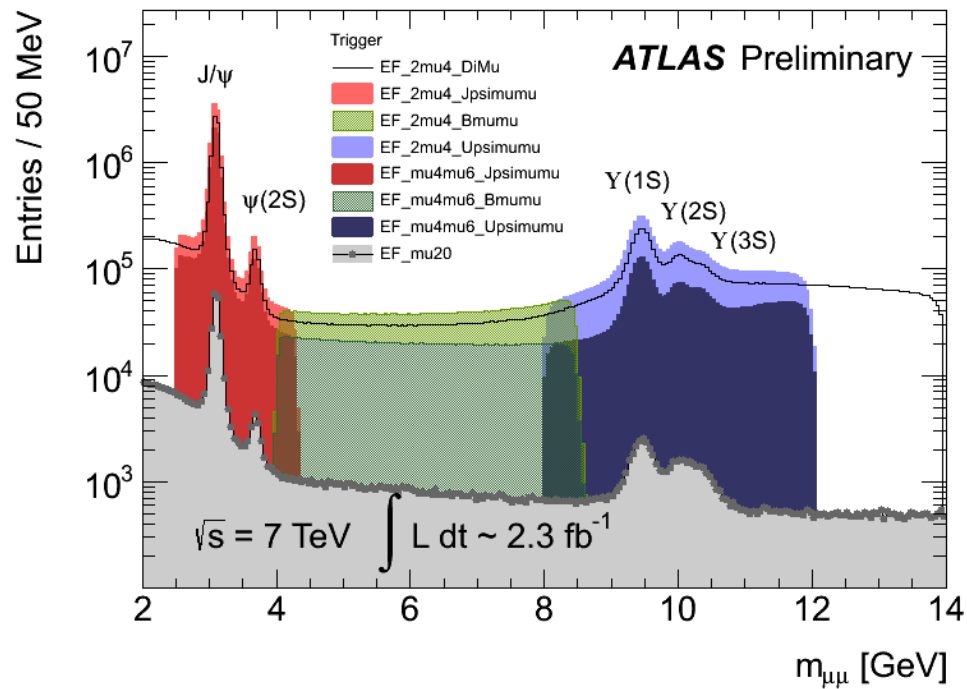
# bb → J/ψ cross section in the fiducial volume

- Signal statistics and background level are important factors in establishing the precision of measurements
- bb → J/ψ and pp → J/ψ cross sections in ATLAS, CMS and LHCb are now measured
- In the ATLAS fiducial volume covered by the 2011 B-triggers the bb → J/ψ cross section is 3 time smaller than LHCb (see table)
- However the (bb → J/ψ)/(pp → J/ψ) is 3.5 times bigger than in LHCb
  - This allows ATLAS to operate without any J/ψ vertex displacement cuts in operation. This is useful for complex lifetime fits.

	Fiducial vol (relevant for Bs → J/ψp)	bb → J/ψ cross section	pp → J/ψ cross section direct cross section	R = bb → J/ψ / pp → J/ψ
ATLAS Nucl. Phys. B 850 (2011) 387-444	p <sub>T</sub> > 7 GeV  y  < 2.4	<b>0.38 ± 0.03 (stat.) ± 0.47 (syst.) ± 0.03 (spin) ± 0.01 (lumi.) μb</b>	0.98 ± 0.02 (stat.) ± 0.13 (syst.) ± 0.15 (spin) ± 0.03 (lumi.) μb	<b>0.39</b>
LHCb Eur. Phys. J. C (2011) 71: 1645	p <sub>T</sub> ∈ [0; 14] GeV y ∈ [2.0; 4.5]	<b>1.14 ± 0.03 (stat.) ± 0.16 (syst.) μb</b>	10.52 ± 0.04 ± 1.40+1.64 μb	<b>0.11</b>



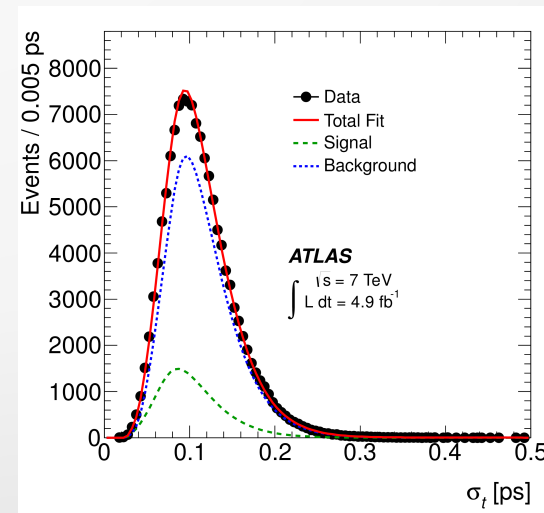
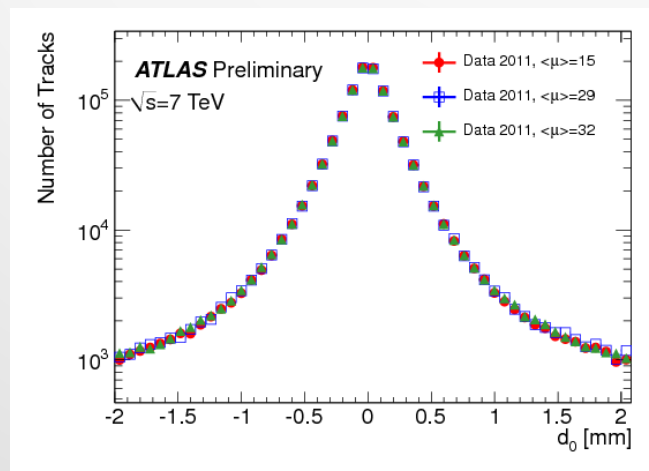
# B-triggers for $J/\psi$



- In 2011 the di-muon triggers with pT thresholds were 4&4GeV or 4&6GeV
- HLT tracking & vertexing, accepting only good quality vertices
- $J/\psi$  trigger rates low – no need for displaced  $J/\psi$  vertex cuts during 2011 and 2012
- With no lifetime cut we have simplified systematics for analysis dependant on lifetime

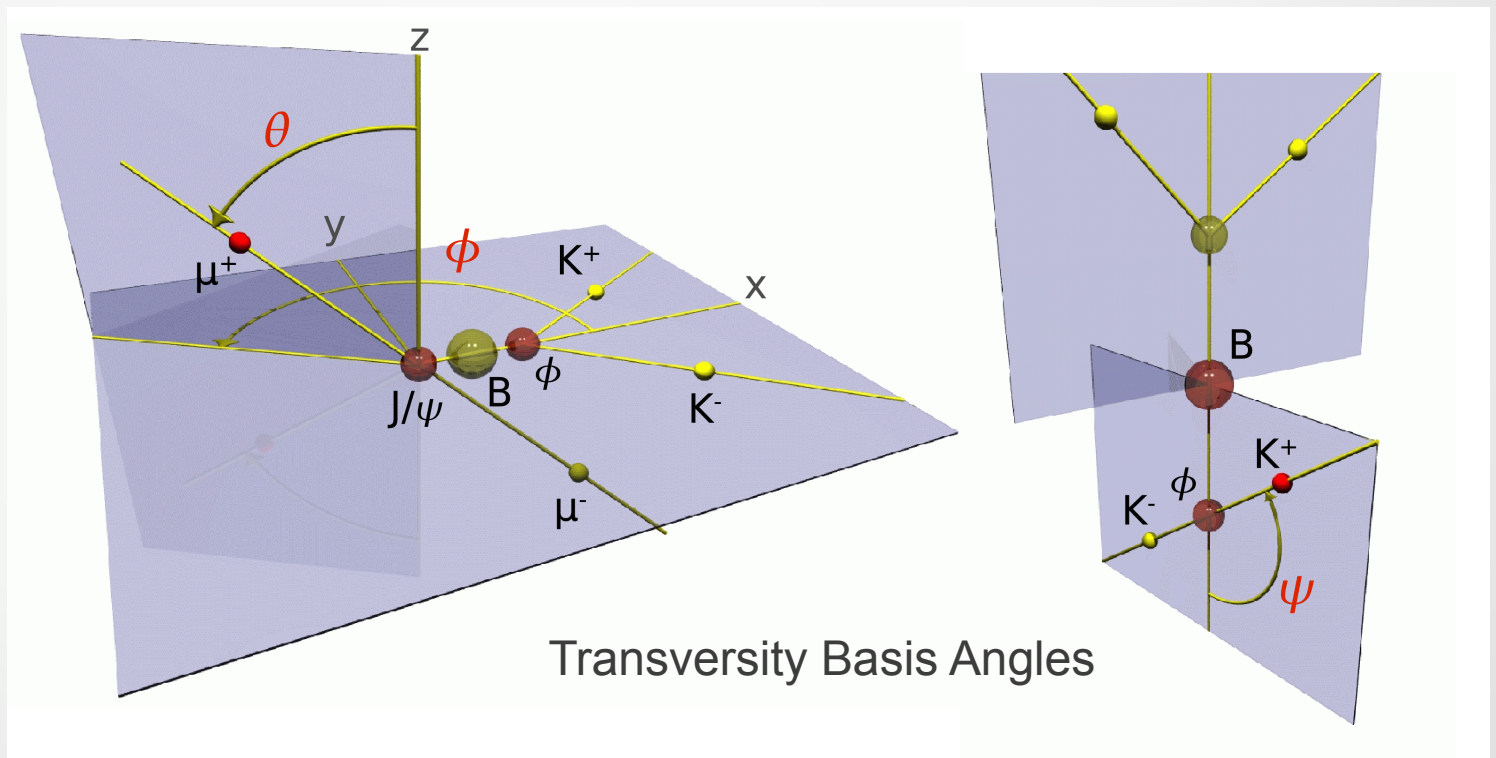
# Time resolution – 2011 Analysis

- Vertex resolution is important for time dependant analyses such as  $B_s \rightarrow J/\psi\phi$
- As pileup increased, quality was measured and resolution remained unchanged
- In 2011 as pileup was increasing, the vertex and d0 reconstruction performance in ATLAS remained stable, which maintained stable time resolution for  $B_s \rightarrow J/\psi\phi$  over all 2011.
- ATLAS average lifetime error was 95 fs for  $B_s \rightarrow J/\psi\phi$





# Time-dependent angular analysis of $B_s \rightarrow J\psi\phi$ , extraction of $\Delta\Gamma_s$ and $\phi_s$



# CP Violation in neutral $B_s$ system

Mixing of flavour eigenstates are governed by:

$$i \frac{d}{dt} \begin{pmatrix} B_s^0(t) \\ \bar{B}_s^0(t) \end{pmatrix} = H \begin{pmatrix} B_s^0(t) \\ \bar{B}_s^0(t) \end{pmatrix} \equiv \left[ \underbrace{\begin{pmatrix} M_0 & M_{12} \\ M_{12}^* & M_0 \end{pmatrix}}_{\text{mass matrix}} - \frac{i}{2} \underbrace{\begin{pmatrix} \Gamma_0 & \Gamma_{12} \\ \Gamma_{12}^* & \Gamma_0 \end{pmatrix}}_{\text{decay matrix}} \right] \begin{pmatrix} B_s^0(t) \\ \bar{B}_s^0(t) \end{pmatrix}$$

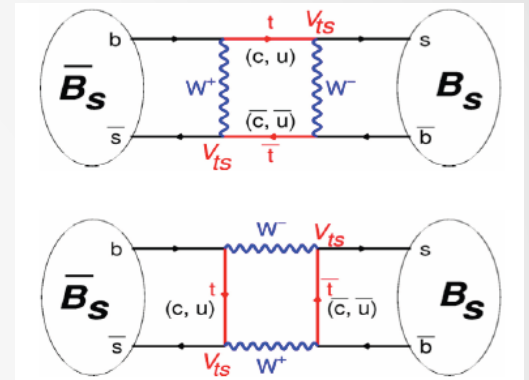
The mass eigenstates

$$\begin{aligned} |B_s^H\rangle &= p |B_s^0\rangle - q |\bar{B}_s^0\rangle \\ |B_s^L\rangle &= p |B_s^0\rangle + q |\bar{B}_s^0\rangle \end{aligned}$$

$$\Delta m_S = m_H - m_L \approx 2|M_{12}|$$

$$\varphi_S^{\text{SM}} = \arg(-M_{12}/\Gamma_{12}) \approx -0.04$$

$$\Delta\Gamma = \Gamma_L - \Gamma_H \approx 2 |\Gamma_{12}| \cos(2 \varphi_S^{\text{SM}})$$



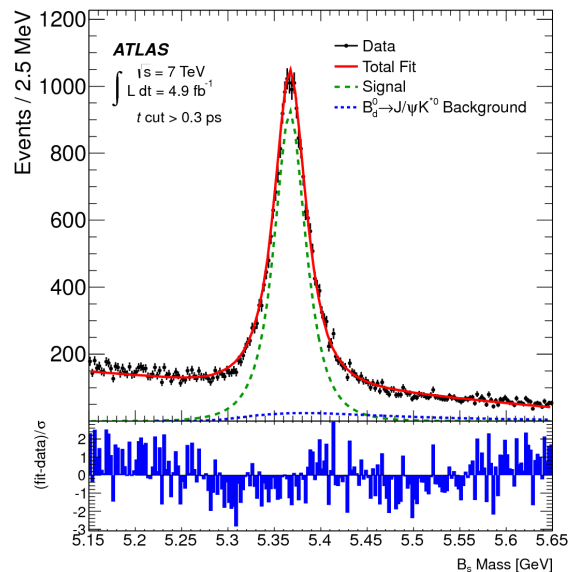
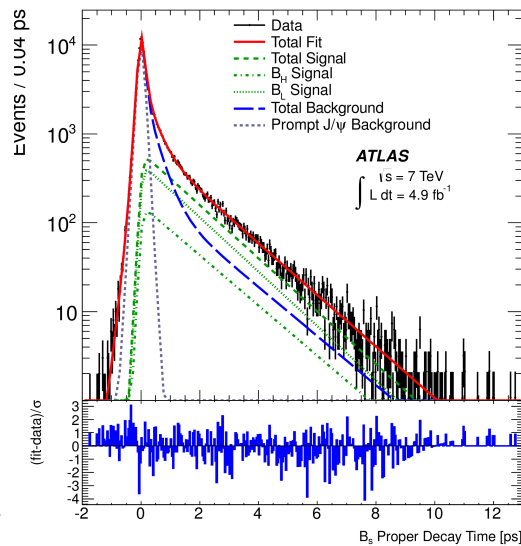
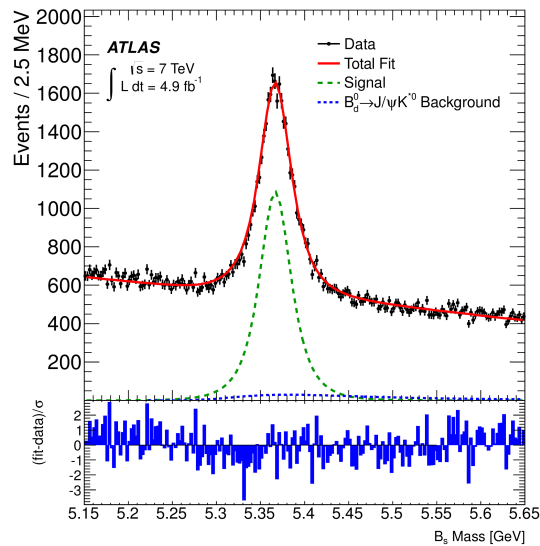
# CP Violation in neutral $B_s$ system

- CP violation can be detected in  $B_s \rightarrow J\psi\phi$  with or without tagging.
- The first analysis is untagged and using the 2011 dataset
- The CP and flavour states were separated statistically through the time-dependence of the decay and angular correlations amongst the final-state particles.
- A tagged analysis makes the measurement more sensitive and will be published in the future

# $B_s \rightarrow J\psi\phi$ System

- $B_s \rightarrow J\psi\phi$  has three spin states of  $J\psi\phi$ , combined into three polarizations amplitudes
  - Longitudinal polarization ( $A_0$ ) CP – even
  - Transverse polarization with the polarization vectors:
    - Parallel ( $A_{\parallel}$ ) CP-even
    - Or perpendicular ( $A_{\perp}$ ) CP-odd
- Another amplitude  $A_S$  is the contribution of CP-odd  $B_s \rightarrow J/\psi K^+ K^- (f_0)$  where the non-resonant  $K^+ K^-$  or  $f_0$  meson is an S-wave state.

# Bs → J/ψφ candidate selection



A proper decay time cut eliminates the direct background but would make the fit systematics more complex

- J/ψ mass window adapted for varying barrel/endcap resolutions
- φ mass window 22 MeV wide
- Kaons  $p_T > 1 \text{ GeV}$
- 4-track B-vertex  $\chi^2/\text{d.o.f.} < 3$
- In total 131k  $B_s$  candidates within  $5.15 < (B_s) < 5.65 \text{ GeV}$  used in the fit
- Number of signal  $B_s$  candidates extracted from the fit  $22690 \pm 160$

# Fit Function

- Unbinned maximum likelihood fit using PDF with signal and two background components

- $$\ln \mathcal{L} = \sum_{i=1}^N \ln(f_s \cdot \mathcal{F}_s(m_i, t_i, \Omega_i) + f_s \cdot f_{B^0} \cdot \mathcal{F}_{B^0}(m_i, t_i, \Omega_i) + (1 - f_s \cdot (1 + f_{B^0})) \mathcal{F}_{\text{bkg}}(m_i, t_i, \Omega_i))$$

- 26 Free parameters extracted from fit
  - 8 physics variables to describe  $\mathbf{B}_s \rightarrow \mathbf{J}/\psi\phi$  and S-wave component:  $\Delta\Gamma_s$ ,  $A_0^2$ ,  $A_1^2$ ,  $\delta_{\parallel}$ ,  $A_s^2$  and  $\delta_s$
- Measured variables:
  - Proper decay time and its error  $t_i$ ,  $\sigma_{t_i}$
  - Mass and its error  $m_i$ ,  $\sigma_{m_i}$
  - Transversity angles  $\Omega_i$  ( $\theta$ ,  $\phi$ ,  $\psi$ )

# Signal pdf

$k$	$\mathcal{O}^{(k)}(t)$	$g^{(k)}(\theta_T, \psi_T, \varphi_T)$
1	$\frac{1}{2} A_0(0) ^2 \left[ (1 + \cos \phi_s) e^{-\Gamma_L^{(s)} t} + (1 - \cos \phi_s) e^{-\Gamma_H^{(s)} t} \right]$	$2 \cos^2 \psi_T (1 - \sin^2 \theta_T \cos^2 \varphi_T)$
2	$\frac{1}{2} A_{  }(0) ^2 \left[ (1 + \cos \phi_s) e^{-\Gamma_L^{(s)} t} + (1 - \cos \phi_s) e^{-\Gamma_H^{(s)} t} \right]$	$\sin^2 \psi_T (1 - \sin^2 \theta_T \sin^2 \varphi_T)$
3	$\frac{1}{2} A_{\perp}(0) ^2 \left[ (1 - \cos \phi_s) e^{-\Gamma_L^{(s)} t} + (1 + \cos \phi_s) e^{-\Gamma_H^{(s)} t} \right]$	$\sin^2 \psi_T \sin^2 \theta_T$
4	$\frac{1}{2} A_0(0)  A_{  }(0)  \cos \delta_{  } \left[ (1 + \cos \phi_s) e^{-\Gamma_L^{(s)} t} + (1 - \cos \phi_s) e^{-\Gamma_H^{(s)} t} \right]$	$\frac{1}{\sqrt{2}} \sin 2\psi_T \sin^2 \theta_T \sin 2\varphi_T$
5	$\frac{1}{2} A_{  }(0)  A_{\perp}(0)  \left( e^{-\Gamma_H^{(s)} t} - e^{-\Gamma_L^{(s)} t} \right) \cos(\delta_{\perp} - \delta_{  }) \sin \phi_s$	$\sin^2 \psi_T \sin 2\theta_T \sin \varphi_T$
6	$-\frac{1}{2} A_0(0)  A_{\perp}(0)  \left( e^{-\Gamma_H^{(s)} t} - e^{-\Gamma_L^{(s)} t} \right) \cos \delta_{\perp} \sin \phi_s$	$\frac{1}{\sqrt{2}} \sin 2\psi_T \sin 2\theta_T \cos \varphi_T$
7	$\frac{1}{2} A_S(0) ^2 \left[ (1 - \cos \phi_s) e^{-\Gamma_L^{(s)} t} + (1 + \cos \phi_s) e^{-\Gamma_H^{(s)} t} \right]$	$\frac{2}{3} (1 - \sin^2 \theta_T \cos^2 \varphi_T)$
8	$-\frac{1}{2} A_S(0)  A_{  }(0)  \left( e^{-\Gamma_H^{(s)} t} - e^{-\Gamma_L^{(s)} t} \right) \sin(\delta_{  } - \delta_S) \sin \phi_s$	$\frac{1}{3} \sqrt{6} \sin \psi_T \sin^2 \theta_T \sin 2\varphi_T$
9	$\frac{1}{2} A_S(0)  A_{\perp}(0)  \left[ (1 - \cos \phi_s) e^{-\Gamma_L^{(s)} t} + (1 + \cos \phi_s) e^{-\Gamma_H^{(s)} t} \right] \sin(\delta_{\perp} - \delta_S)$	$\frac{1}{3} \sqrt{6} \sin \psi_T \sin 2\theta_T \cos \varphi_T$
10	$-\frac{1}{2} A_0(0)  A_S(0)  \sin(-\delta_S) \left( e^{-\Gamma_H^{(s)} t} - e^{-\Gamma_L^{(s)} t} \right) \sin \phi_s$	$\frac{4}{3} \sqrt{3} \cos \psi_T (1 - \sin^2 \theta_T \cos^2 \varphi_T)$

- In an untagged analysis terms 5 and 6 are multiplied by a small factor of  $\sin(\varphi_s)$ . Thus the analysis is not sensitive to  $\delta_{\perp}$ 
  - A gaussian constraint to the best measured value (LHCb [arXiv:1112.3183]),  $\delta_{\perp} = (2.95 \pm 0.39)$  rad applied
- Acceptance corrections for angular sculpting of the detector and kinematic cuts included in the signal PDF
  - 4D binned acceptance maps calculated from the  $B_s \rightarrow J/\psi \phi$  MC events
  - Corrections applied on event-by-event basis according to  $(\theta, \psi, \varphi)$  and  $p_T$  of  $B_s$  signal candidate

# Background representation in the fit

- Time component of background:
  - Prompt background: delta function at 0, convoluted by Gauss **per-candidate resolution**  $\sigma_{ti}$
  - Two exponentials representing longer-lived backgrounds
  - Small negative exponential component for events with poor vertex resolution
- Background angular shapes
  - Arise from detector and kinematic sculpting
  - Described by empirical functions with parameters determined in the fit simultaneously with 26 parameters
- Background mass model – linear function
- $B^0 \rightarrow J/\psi K^{*0}$  and  $B^0 \rightarrow J/\psi K\pi$  contamination treated separately
  - fractions  $(6.5 \pm 2.4)\%$  and  $(4.5 \pm 2.8)\%$  determined from MC
  - mass, angular shapes - from MC
  - used in PDF but no free parameters of fit



# $B_s \rightarrow J/\psi\phi$ results

	$\phi_s$	$\Delta\Gamma_s$	$\Gamma_s$	$ A_0(0) ^2$	$ A_{  }(0) ^2$	$ A_S(0) ^2$
$\phi_s$	1.00	-0.13	0.38	-0.03	-0.04	0.02
$\Delta\Gamma_s$		1.00	-0.60	0.12	0.11	0.10
$\Gamma_s$			1.00	-0.06	-0.10	0.04
$ A_0(0) ^2$				1.00	-0.30	0.35
$ A_{  }(0) ^2$					1.00	0.09
$ A_S(0) ^2$						1.00

Parameter	Value	Statistical uncertainty	Systematic uncertainty
$\phi_s(\text{rad})$	0.22	0.41	0.10
$\Delta\Gamma_s(\text{ps}^{-1})$	0.053	0.021	0.010
$\Gamma_s(\text{ps}^{-1})$	0.677	0.007	0.004
$ A_0(0) ^2$	0.528	0.006	0.009
$ A_{  }(0) ^2$	0.220	0.008	0.007
$ A_S(0) ^2$	0.02	0.02	0.02

The PDF is invariant under the transformation:

$$\{\varphi_s, \Delta\Gamma_s, \delta_{\perp}, \delta_{||}, \delta_s\} \rightarrow \{\pi - \varphi_s, \pi - \Delta\Gamma_s, \pi - \delta_{\perp}, -\delta_{||}, -\delta_s\}$$

In absence of tagging it is also invariant:

$$\{\varphi_s, \Delta\Gamma_s, \delta_{\perp}, \delta_{||}, \delta_s\} \rightarrow \{-\varphi_s, \Delta\Gamma_s, \pi - \delta_{\perp}, -\delta_{||}, -\delta_s\}$$

Leading to fourfold ambiguity

We constrain  $\delta_{\perp}$  to the result from LHCb tagged analysis so only the positive  $\varphi_s$  solution is kept

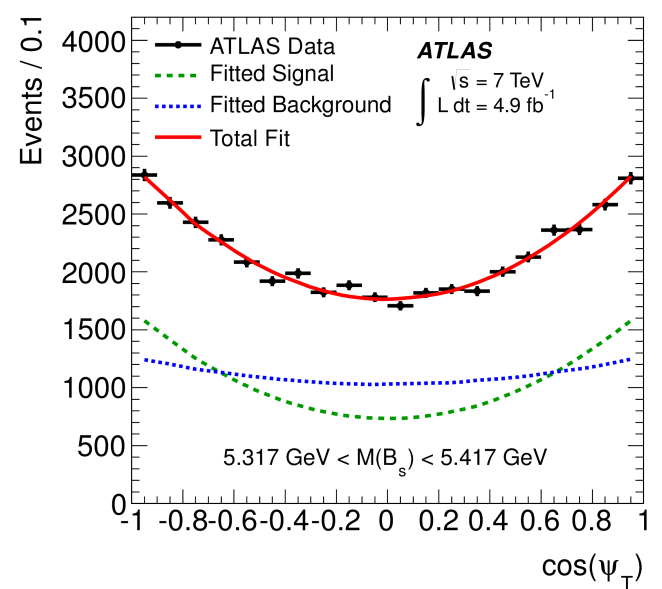
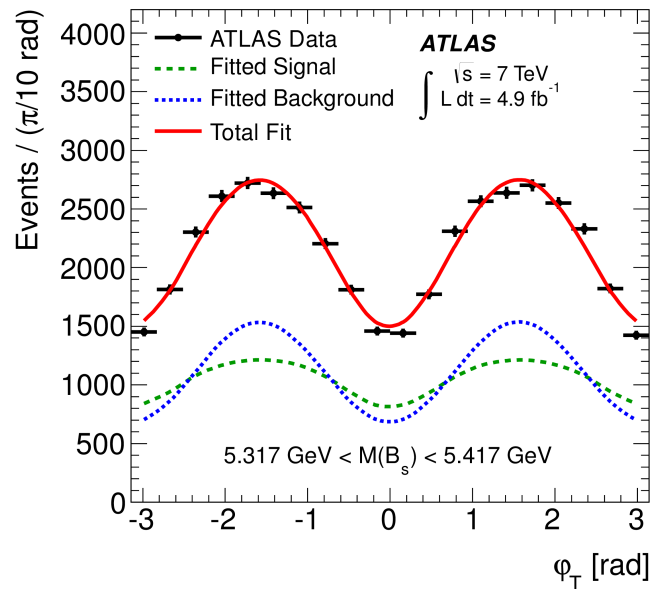
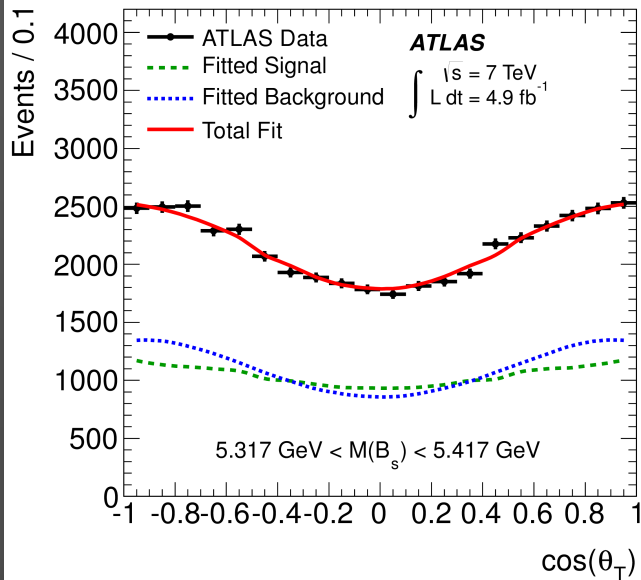
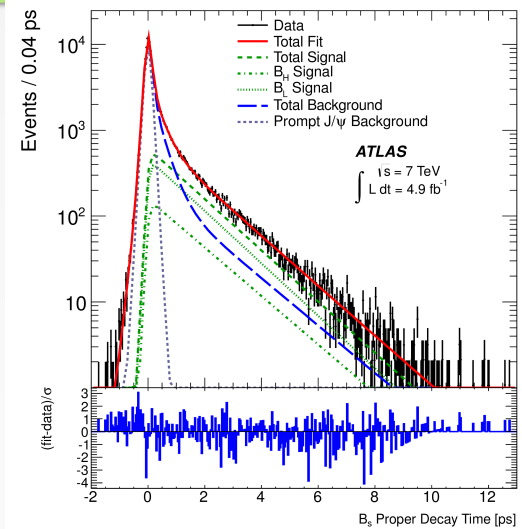
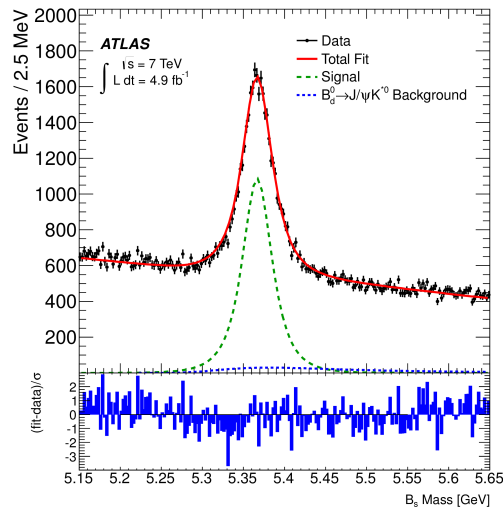
The solution with a negative  $\Delta\Gamma_s$  is excluded using another LHCb measurement which determines the  $\Delta\Gamma_s$  to be positive

# Systematic uncertainties

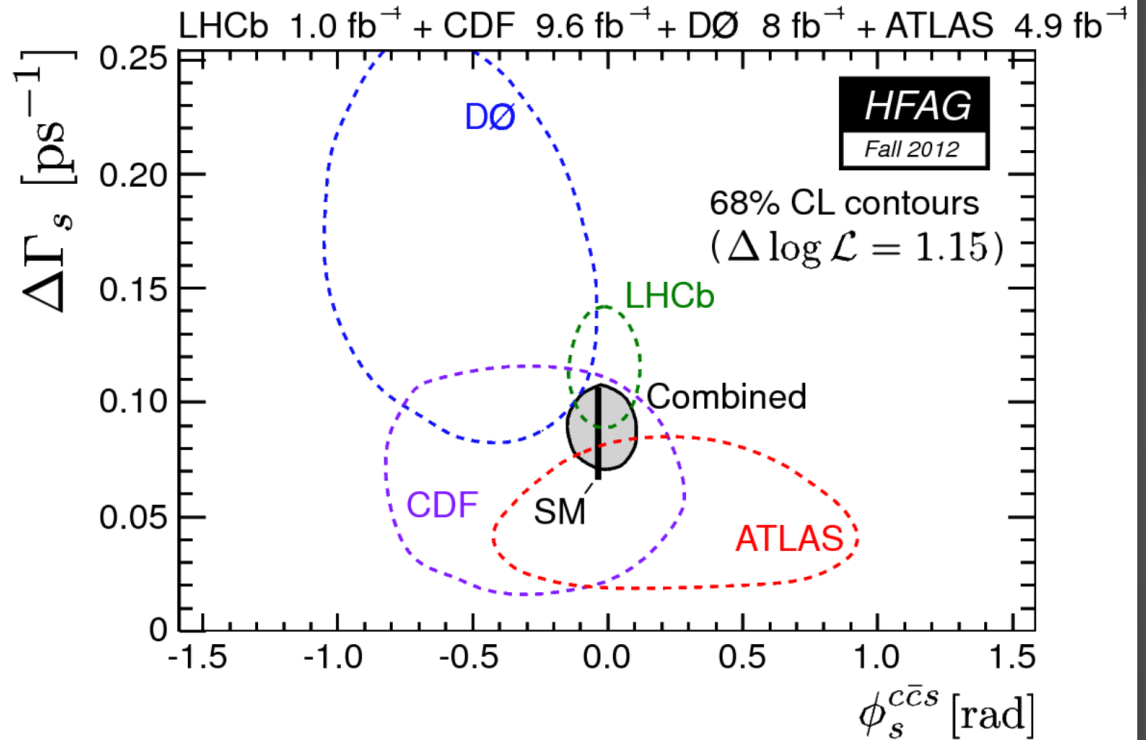
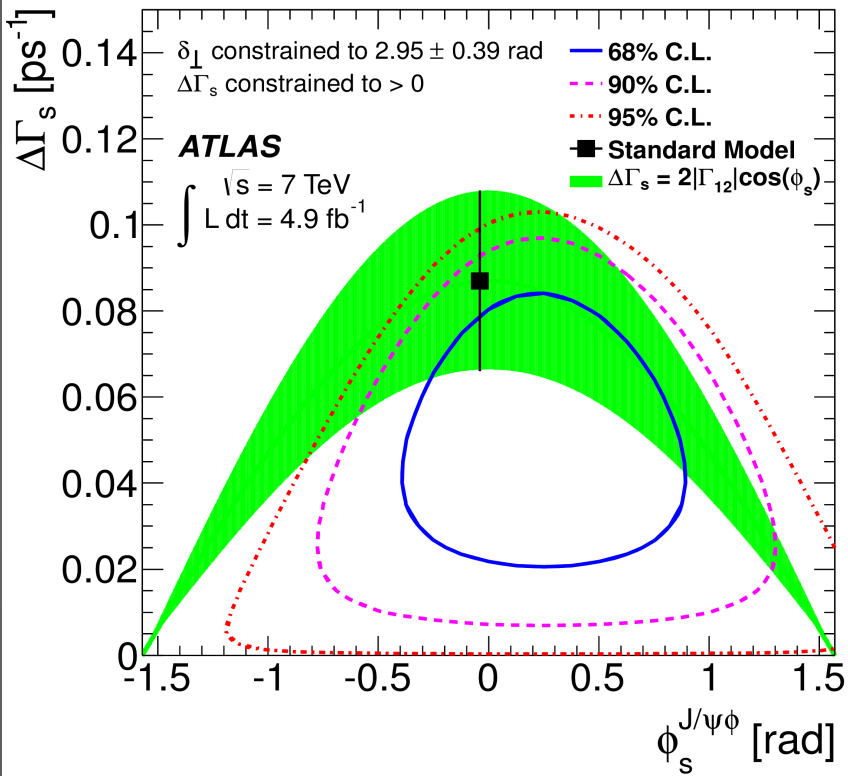
Systematic Uncertainty	$\phi_s(\text{rad})$	$\Delta\Gamma_s(\text{ps}^{-1})$	$\Gamma_s(\text{ps}^{-1})$	$ A_{\parallel}(0) ^2$	$ A_0(0) ^2$	$ A_S(0) ^2$
Inner Detector alignment	0.04	< 0.001	0.001	< 0.001	< 0.001	< 0.01
Trigger efficiency	< 0.01	< 0.001	0.002	< 0.001	< 0.001	< 0.01
Default fit model	< 0.001	0.006	< 0.001	< 0.001	0.001	< 0.01
Signal mass model	0.02	0.002	< 0.001	< 0.001	< 0.001	< 0.01
Background mass model	0.03	0.001	< 0.001	0.001	< 0.001	< 0.01
Resolution model	0.05	< 0.001	0.001	< 0.001	< 0.001	< 0.01
Background lifetime model	0.02	0.002	< 0.001	< 0.001	< 0.001	< 0.01
Background angles model	0.05	0.007	0.003	0.007	0.008	0.02
$B^0$ contribution	0.05	< 0.001	< 0.001	< 0.001	0.005	< 0.01
<b>Total</b>	0.10	0.010	0.004	0.007	0.009	0.02

- Systematics dominated by modelling background angular distributions.

# Fit Projections

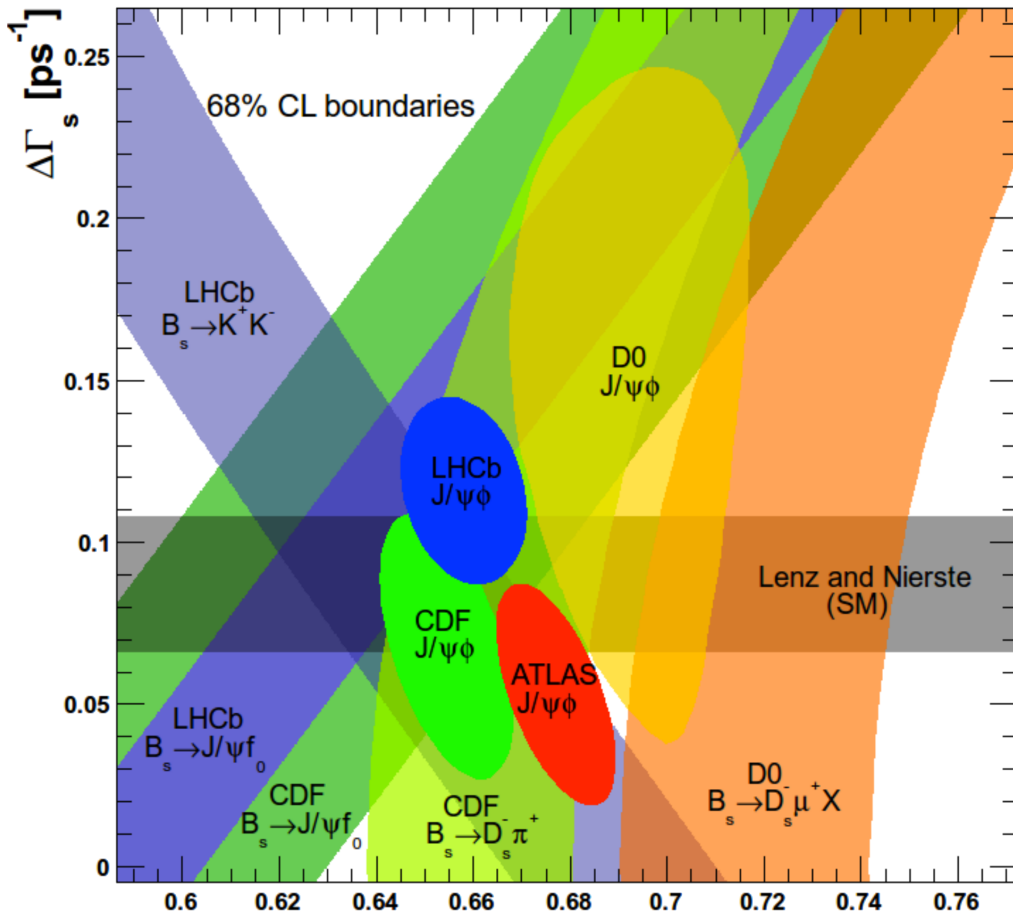


# Comparison with other results



The inclusion of the ATLAS measurement brings the world average closer to the Standard model prediction  
 Note all other experiments are shown with tagging leading to better accuracy on  $\phi_s$

# Summary of $\Gamma_s$ and $\Delta\Gamma_s$ measurements



Note: CMS has a similar analysis ( $B_s \rightarrow \Gamma_s [ps^{-1}]$   $J/\psi\phi$ ) but with  $\phi_s$  fixed - CMS-PAS-BPH-11-006

30/11/12

$B_s \rightarrow J/\psi\phi$  results from four experiments overlaid with constraints from  $B_s \rightarrow J/\psi f^0$ ,  $B_s \rightarrow K^+K^-$ ,  $B_s \rightarrow D_s\pi$  and  $B_s \rightarrow D_s\mu X$  analyses.

The shapes for  $B_s \rightarrow J/\psi\phi$  are constructed by summing the statistical and systematic errors in quadrature and using the correlation coefficient from multi-dimensional fit.

$B_s \rightarrow J/\psi f^0$  bands (assuming  $\phi_s = 0$ ); Results are consistent with SM

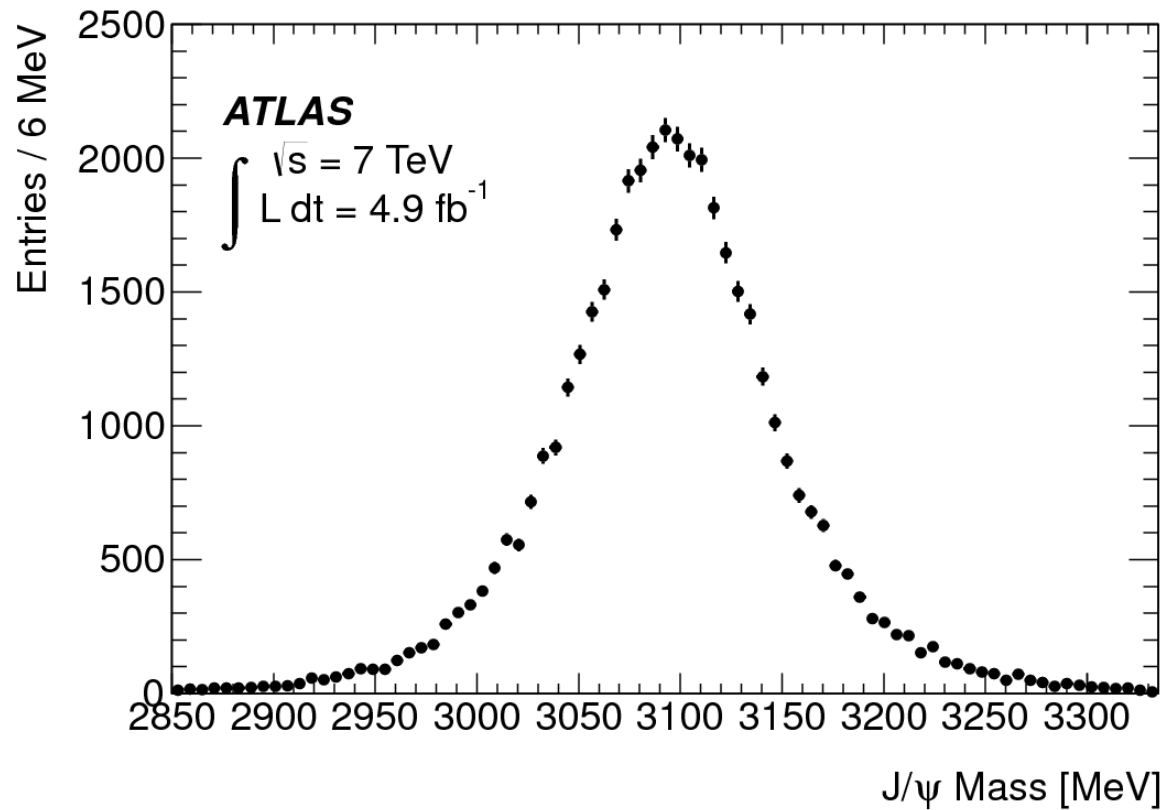
ATLAS, arXiv:1208.0572;  
 LHCb-CONF-2012-002;  
 CDF note 10778;  
 D0, PRD85, 032006 (2012);  
 LHCb, arXiv:1207.0878;  
 CDF, PRD84, 05012 (2011);  
 LHCb, arXiv:1207.5993;  
 K. De Bruyn et al., arXiv:1204.1735;  
 CDF, PRL 107:272001(2011);  
 D0, PRL 97, 241801 (2006);  
 Lenz and Nierste, arXiv:1102.4274

# Conclusions

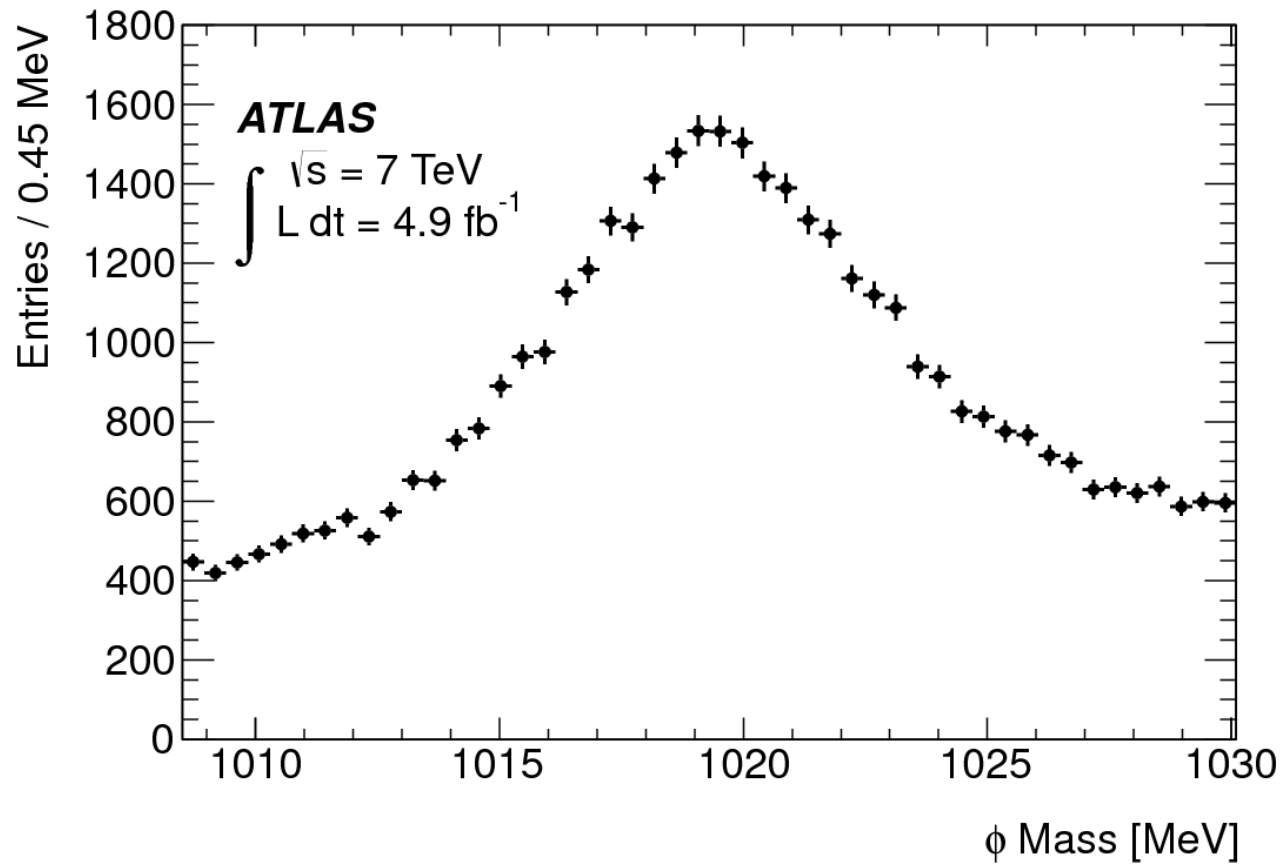
- ATLAS has performed a measurement of CP violation in decay  $B_s \rightarrow J/\psi\phi$  using untagged time-angular analysis of 4.9 fb<sup>-1</sup> data collected in 2011
- Several parameters describing the  $B_s$  system are measured including the mean  $B_s$  lifetime, the decay width difference  $\Delta\Gamma_s$ , the transversity amplitudes  $|A_0(0)|$  and  $|A_{\parallel}(0)|$  and the weak phase  $\varphi_s$ .
- Analysis will be refined, tagging included and 2012 data added

# Back up Slides

# Jpsi Mass plot







# Prospects

- Statistical error will be improved by incorporating the 2012 dataset.
- Tagged analysis will be added improving even the 2011 data
- Analytical methods will be refined to try and reduce systematic error
- High luminosities and trigger adjustments will mean a more events will be at higher  $p_T$  which marginally improves vertex resolution